Overload effects on local fatigue crack-tip strain fields in plane stress samples

P. J. Withers, H. Dai, P. Lopez-Crespo♣
School of Materials, University of Manchester, Grosvenor Street, Manchester M1 7HS, UK

A. Steuwer
ESS Scandinavia, University of Lund, 22350 Lund, Sweden
NMMU, Gardham Avenue, Port Elizabeth 6031, South Africa

F. Yusof
School of Mechanical Engineering, Universiti Sains Malaysia, Nibong Tebal 14300, Penang, Malaysia

J. F. Kelleher
ISIS, Rutherford Appleton Laboratory, Didcot, Oxfordshire OX11 0QX, UK

T. Buslaps
ESRF, 6 rue J Horowitz, 38000 Grenoble, France

ABSTRACT. Conventional linear elastic fracture mechanics (LEFM) provides a rigorous basis for analysing sub-critical crack growth in terms of parameters (e.g. stress intensity factor (K), CTOD, J) that capture the local conditions at the crack-tip, yet can be determined solely in terms of external, macroscopic loading and geometrical parameters. However in many cases (e.g. for variable loading) the stress at the crack-tip cannot easily be inferred solely from a global approach and local information is required. The advent of 3rd generation synchrotron facilities has opened up the possibility of measuring local crack-tip strains under both plane strain and plane stress. In this work, the behaviour of the crack-tip before, during, immediately after an overload event is examined for fatigue cracks in thin (plane stress) stainless steel CT specimens. X-ray diffraction has revealed large compressive residual stresses ahead of the crack, but no evidence for plasticity induced closure behind the crack-tip.

KEYWORDS. Overload effect; Synchrotron X-ray diffraction.

INTRODUCTION

In the past three decades, our knowledge of fatigue mechanisms improved considerably and as a consequence, different tools for predicting crack growth rates have been proposed. However, there are still issues to be resolved [1]. For example, there are a number of uncertainties relating to crack closure which is commonly used to explain

♣ Now at: *Department of Civil and Materials Engineering, University of Malaga, C/Dr Ortiz Ramos s/n, 29071 Malaga, Spain*

overload retardation [2]. Plasticity induced crack closure is one of the most important mechanisms of crack closure, but its effect is still the subject of on-going debate. Some researchers believe that closure does not occur at all [3], others believe that it can only occur under plane stress [4]. Retardation effects have also been ascribed to residual stresses thus induced [5, 6], crack blunting [7], and crack deflection [8]. To date, experimental measurements of crack closure have been inconclusive and have relied on either (i) measuring some secondary property of the cracked body such as compliance or electrical resistance or (ii) measurement of crack-opening displacements on the surface of the cracked body. There are significant difficulties interpreting secondary data in terms of crack-tip stresses. Whilst the surface of a cracked body experiences conditions of plane stress, the bulk can experience conditions more akin to plane strain. The transition in closure effects between plane stress and plane strain conditions has not been fully resolved because of the difficulty of conducting measurements through the volume in most engineering materials. Accordingly, until recently the bulk of the material has only been studied by means of numerical methods [9, 10]. The recent emergence of high brilliance, hard X-ray beamlines at 3rd generation synchrotron sources allow elastic strain to be mapped deep within test-pieces at resolutions (~25μm) limited essentially by the grain size of the sample [11-13]. Here this technique is employed to study the effect of an overload cycle in the crack-tip field in plane stress. Due to beam time constraints, bulk measurements were only performed just before the overload, during the overload and immediately after the overload. Results for the corresponding plane strain case will be reported at a later date.

EXPERIMENTAL DETAILS

Material and specimen

The material employed was 316L stainless steel whose chemical composition is shown in Tab. 1. The standard compact tension (CT) specimen geometry described in ASTM [14] was employed. The thickness of the specimen was 3 mm.

Alloy	C	Si	Mn	P	S	Cr	Ni	Mo	Co	Cu	N	Ti
316L	0.023	0.528	1.570	0.030	0.026	16.72	10.01	2.04	0.163	0.532	0.048	0.001

Table 1: Chemical composition in % of 316L stainless steel. The balance is Fe.

Fatigue crack growth data

The effect of an overload was evaluated on two samples. Initially, the fatigue cracks were grown (~87,000 cycles) to eliminate the sharp starter notch effect following ASTM 647 by about 9 mm giving a crack length of a = 19 mm, as defined in [14]. For the first sample a single 100% overload cycle was applied. After this ~160,000 further cycles were applied at a frequency of 10 Hz at a load ratio, R = 0.05 and constant load, ΔP = 2.1 kN. Accordingly, the stress intensity factor range, ΔK, increased as the crack grew. Fig. 1 shows measurements of the crack growth rate made by direct observation of the crack on the surface by travelling microscope. A drastic change in the growth rate is evident in Fig.1 at point *d* at which point the stress intensity was raised from 21.4 MPa√m (K_{max}) to 43.9 MPa√m ($2K_{max}$) for one cycle before returning to the original level. After a short period of accelerated growth (d to e) an extended period of retarded growth was observed in common with previous experiments [2, 6]. The slope of the curve is much higher before the overload was applied, meaning that crack growth was faster before the overload. The growth rate did not recover to the original rate until some 100,000 cycles after the overload.

X-ray diffraction experimental setup

The crack-tip strain fields were measured on the ID15A beamline at the European Synchrotron Radiation Facility (ESRF), Grenoble, for the second sample using the same arrangement as that described in [13] shown schematically in Fig.2. Three fatigue cycles were observed; one just before overload (OL-1), one during overload (OL) and one immediately after (OL+1). The crack-tip strain field was recorded at peak load and during progressive unloading to K_{min} for each fatigue cycle. The load was first increased to a maximum value and was maintained so that the X-ray measurement was performed. The incident beam slits were opened to 500 ×500 μm giving a gauge length through-thickness of around 11.45 mm (i.e. the full sample thickness was sampled).

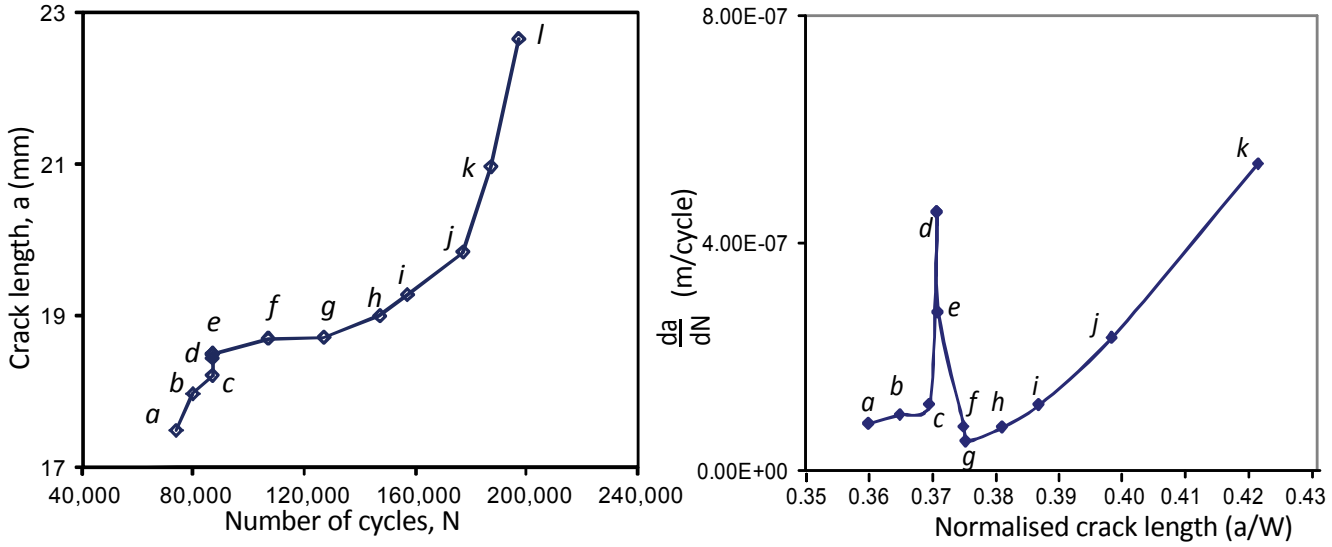

Figure 1: a) Crack length evolution as a function of the number of applied cycles, b) da/dN as a function of normalised crack length. A single cycle 100% overload was applied at point *d*.

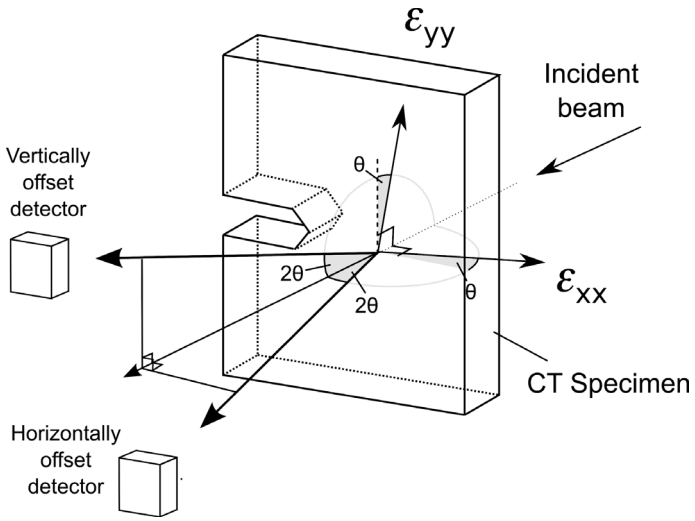

Figure 2: Schematic of the diffraction geometry showing a CT specimen with the crack plane horizontal, and the two detectors measuring two directions of strain; note the coordinate system for ε_{xx} and ε_{yy} adopted (after [13]).

RESULTS

The results of measuring the crack opening strain (ε_{yy}) along the crack plane ($y = 0$) line with the gauge centred on the mid-plane ($x = 0$) are shown in Fig. 2. Unfortunately, the measured elastic strains exhibit considerable point-to-point scatter (~5×10^{-4}) which is much larger than the diffraction peak fit scatter (~10^{-5}). This is attributed to grain size scatter [15] and was reproducible if the scan were repeated. In the following figures (Figs. 3-5) the strain field is shown relative to the position of the crack $x = 0$ and this corresponds to a distance some 18.5 mm from the mouth of the notch (see Fig. 1a) as compared to the surface crack-tip that was recorded as being at 19 mm.

Many interesting features are observed in Fig. 3. Prior to overload (OL-1) (Fig. 3a), the crack is clearly discerned despite the point to point scatter. The strains in the crack wake are, as one would expect, nearly zero. Upon decreasing the load from K_{max}, the elastic strains fall ahead of the crack-tip, especially within 3mm. It is also clear that the crack-tip strain falls to become compressive from a load of around $0.3K_{max}$ with a compressive zone extending around 700 μm ahead of the

crack at K_{min}. It would appear that the compressive region lies predominantly ahead of the crack rather than behind it indicating that the residual stress arises from plasticity ahead of the crack rather than to crack closure behind it.

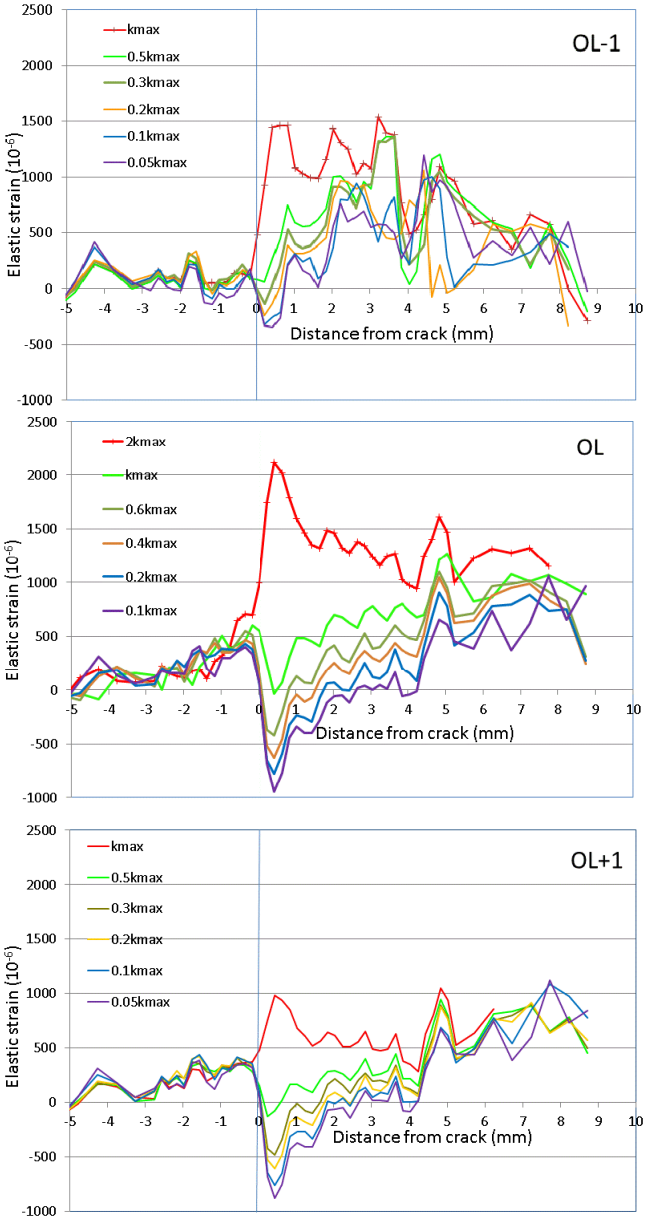

Figure 3: Crack opening elastic strain (ε_{yy}) evolution with the gauge centred at the mid-plane (t = 1.5 mm) along the crack. The crack-tip is located at $x = 0$ mm and the crack mouth is towards negative x coordinates. Elastic strain profiles are shown for the cycle just before the overload (a), during the overload cycle (b) and for the cycle just after the overload (c). The crack $x = 0$ is recorded as 18.5 mm from the notch.

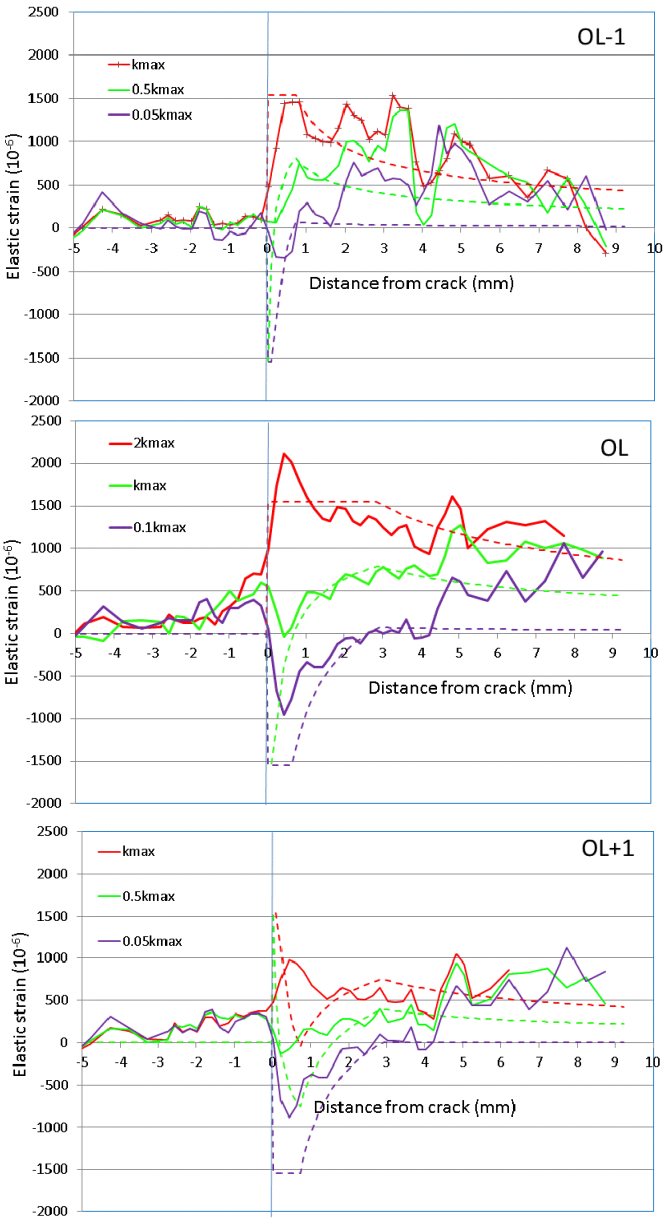

Figure 4: Elastic strain (in 10^{-6}) evolution at the mid plane (t = 1.5 mm) along the crack. Strain curves measured and predicted by modified Westergaard's solutions (dashed) are shown on all plots. Profiles are shown for the cycle just before the overload (a), during the overload cycle (b) and for the cycle just after the overload (c).

Unsurprisingly, the crack-tip strain is significantly larger at overload (Fig.3b). It should be observed that upon unloading from the overload the crack-tip strain is already compressive by the time the load reaches the usual maximum fatigue load (K_{max}). This is due presumably to plasticity just ahead of the crack at overload. The extent of the compressively strained region grows with further unloading until it has extended some 2700 μm ahead of the crack-tip at K_{min}. As regards the first cycle after the overload, (OL+1), it is clear form Fig. 3c that some reverse plastic flow must have occurred upon

unloading from $2K_{max}$ because the stress field at K_{max} on reloading is not the same as it was during unloading from $2K_{max}$. By contrast it is clear from the fact that at K_{min} the curves for OL+1 and for OL almost coincide suggest that the cycle immediately after OL is predominantly an elastic one. It would appear that the strain is significantly tensile at around 7 mm for all the loads for the three fatigue cycles. This observation is surprising and could be due to residual stresses in the original plate, or due to long range stresses introduced during the fatigue cycling. Finally it should be noted that because the gauge volume was 11.45 mm through-thickness and 0.5 mm laterally the gauge samples a significant volume both in terms of any through-thickness variation in stress and in terms of lateral averaging.

DISCUSSION

Taking a very simple approach assuming plane stress conditions across the volume scanned, the plastic zones, in forward (r_p) and reverse (r_c) straining are given by [16]:

$$r_p = \frac{1}{2\pi}\left(\frac{K_I}{\sigma_y}\right)^2 \qquad r_c = \frac{1}{2\pi}\left(\frac{K_I}{2\sigma_y}\right)^2 \tag{1}$$

where σ_y is the yield stress. Rice stated that in practice the zone will be twice this due to load redistribution [7]. The question then arises as to what value of yield stress should be used? The yield stress of 316 stainless is typically around 300 MPa, while significant work hardening leads to an ultimate tensile stress of around 600 MPa. According to Rice, the initial yield stress would give forward and reverse plastic strains of 1620 and 405 μm while the UTS would give zones of 405 and 101 μm respectively. Further in view of the equi-biaxial stress along the crack-tip plane predicted by the Westergaard's solutions [17], these equate to yielding at elastic strains of around of around 1030 and 2060 $\times 10^{-6}$ respectively. One might expect of yield stress of 300 MPa to represent a lower bound estimate, given the opportunity for cyclic hardening during the 87,000 cycles needed to grow the crack to this position. In the following discussion a value of 450 MPa has been chosen and this is supported by the fact that much larger strains than 1000×10^{-6} are observed in Fig. 3 (suggesting 300 MPa is too small), while using a value near to the UTS for yielding would appear to give unrealistically small plastic zones. This intermediate value gives forward and reverse plastic zones of 720 and 180μm at K_{max} and 2880 and 720 μm at $2K_{max}$. A simple biaxial analysis based on Westergaard's solutions, but modified to account of plastic deformation when a stress of 450 MPa is exceeded (strain $>1545 \times 10^{-6}$) and the associated load redistribution needed to give the larger plastic zones predicted by Rice are shown in Fig. 4. Of course there are the issues of progressive work-hardening over successive cycles and the Bauschinger effect on reversing the direction of straining to consider, but the current results exhibit too much point to point scatter to merit anything other than a relatively simple analysis.

It is clear by comparing the measured strains with the predictions that the measured strains broadly agree with the predictions, but there are some interesting discrepancies too. These can also be better understood if the unloading responses are also considered relative to that recorded for K_{min} after unloading for each of the 3 successive cycles (Fig 5). Firstly, the predicted curves upon loading to K_{max} (Fig 4a) suggest plasticity would arise within 700 μm ahead of the crack-tip. This is in reasonable agreement with the experimental results given the large point to point scatter. Upon unloading this is predicted to cause a compressively stressed plastic zone extending to around 700 μm from the crack. This is also in good agreement with the observations, but the magnitude of the compressive stress is much smaller than the simple analysis predicts, being around 300×10^{-6} as against -1500×10^{-6}. To some extent this may be because the gauge volume averages over a considerable distance laterally (~500 μm) smoothing out the sharp trough, but the stress still appears rather small. The fact that the stresses predominantly elastically unload is confirmed by Fig. 5a, for which the change as K is reduced is well matched to the predictions, except within 500 μm of the tip for which the strains appear to be significantly smaller than expectation. This could be because of the smearing effect of the gauge, or the Bauschinger effect or some other effect.

The results for recorded for the 100% overload are again in approximate agreement with the simple model (Fig. 4b) pointing to extensive plasticity extending to around 3mm from the crack-tip. Upon unloading significant reduction in stress is observed. That this is primarily an elastic unload can be inferred from Fig. 5b, however it is clear that the strains within 3 mm of the crack-tip are generally smaller than predicted from an elastic unload. The fit to the simple predictions in this case are poor, largely because the compressive strains in front of the crack are some $500\text{-}600 \times 10^{-6}$ smaller than

predicted upon unloading from overload. This means that the strains upon reloading during OL+1 are correspondingly more tensile than would otherwise occur (Fig. 3c).

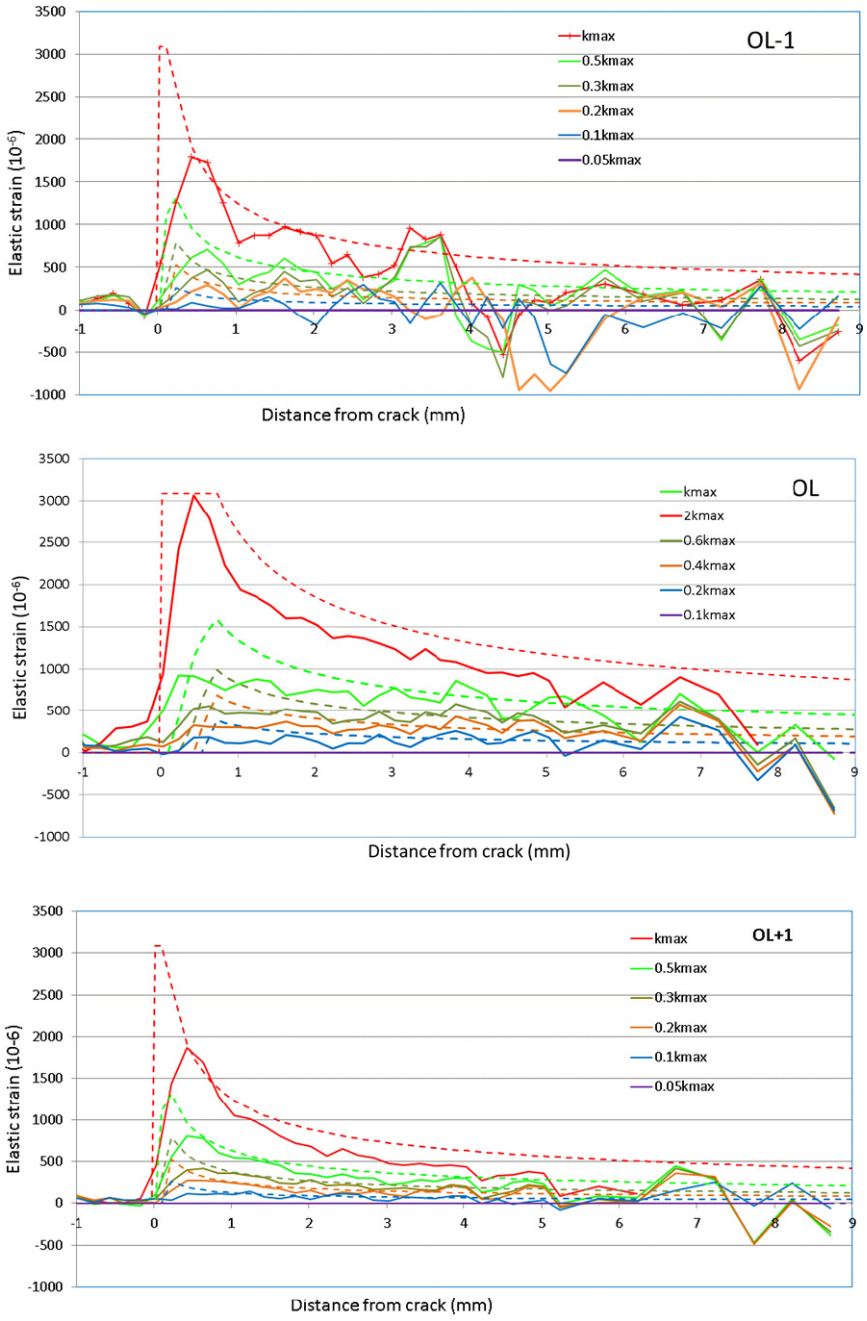

Figure 5: The elastic strain (ε_{yy}) evolution at the mid-plane (t = 1.5 mm) along the crack relative to the next K_{min} profile (i.e. K-K_{min}). Strain curves measured and predicted (dashed) by modified Westergaard's solutions are shown on all plots. Profiles are shown for the cycle just before the overload (a), during the overload cycle (b) and for the cycle just after the overload (c).

It should be noted in all three cycles the strains behind the crack are essentially unchanged during the loading cycles as is evident in Fig. 4. This might suggest a lack of closure across the crack faces as load is reduced towards K_{min}. While one would not expect closure for the overload and OL+1 cycles due to the plastic crack-tip blunting achieved by the overload event, one might expect plasticity induced closure prior to the OL give the large plastic zone; however the low level of closure may in part be due to the progressive increase in K experienced by the crack as it grows.

For the subsequent normal fatigue cycle (OL+1) the initial compressive strain ahead of the crack-tip means that the peak strain is not very pronounced (Fig. 4c). However it is larger than when the applied stress reached K_{max} on the previous unload (Fig. 4b). This shows that the region ahead of the crack-tip did undergo some reverse plasticity on unloading from the overload (Fig. 5b). By contrast, the OL+1 cycle is essentially elastic as confirmed both by the fact that the strain field at K_{min} maps almost exactly (point to point scatter included) to the K_{min} field for the previous cycle and by the close to elastic unloading response in Fig. 5c (except for within 500μm of the crack-tip).

CONCLUSIONS

The results showed in this work attempt to characterise the effect of a single overload on the crack-tip field in the middle of a thin (plane stress) specimen. To obtain a more complete picture of the crack-tip strain field requires additional strain data at the surface, which will be obtained by means of digital image correlation (DIC); which is the subject of a subsequent study [18] for which the crack is grown through both the acceleration zone (where closure effects are expected to be small) and the retardation zone. Initial indications from that work support a traditional plasticity induced closure interpretation showing a knee in the closure response prior to overload, an absence of closure in the accelerated growth regime followed by accentuated closure in the retardation regime. However plasticity induced crack closure is not evident in the current results. Perhaps somewhat surprising, given the state of almost plane stress and the extensive plasticity, no direct evidence for plasticity induced crack closure is observed for any of the three cycles. This is unusual for the OL-1 case; it may be because closure occurs near the surfaces (as would be recorded by DIC) which causes the centre to be held open remotely; certainly there is no sign of crack face compression. The fact that K is increasing slowly with crack growth may in part explain this – though that would leave the knee in the crack opening recorded by complementary DIC results to explain. Instead, these measurements taken with a relatively large gauge volume appear to show extensive plasticity induced residual stresses which in turn strongly influence the crack-tip stress field.

In a previous publication it was possible to infer the stress intensity factor acting at the crack-tip by fitting the measured strains to analytical solutions [13]. Here the measured strains have been directly compared with Westergaard's analytical solution which was only modified to take into account the plasticity and the associated redistribution of that load. These predictions broadly correspond to the measured strains. The forward and reverse plastic zones are predicted well by this approach if a value of the yield stress intermediate between the initial yield stress and the ultimate tensile stress is used. This suggests that cyclic hardening is important. However the strains within 500 μm of the crack-tip appear to be consistently smaller than anticipated, both in tension and compression. This may be due to the extended gauge volume which samples strains over a significant length-scale, potentially smearing out the sharp crack tip. Equally, the crack-tip is not linear across the sample width. To take this investigation further, the experiment will be repeated on finer grained materials where both higher spatial resolution and more accurate strain fields would be obtained.

ACKNOWLEDGEMENTS

The authors are grateful to the ESRF for the beamtime and support in operating ID15A.

REFERENCES

[1] M. N. James, In: Advances in Fracture Research, Proceedings of the Ninth International Conference on Fracture, B. L. Karihaloo editor, Sydney, Australia: Pergamon Press (1996).
[2] C. S. Shin, S. H. Hsu, International Journal of Fatigue, 15 (1993) 181.
[3] K. Sadananda, A. K. Vasudevan, R. L. Holtz, E. U. Lee, International Journal of Fatigue, 21 (1999) S233.
[4] H. Alizadeh, D. A. Hills, P. F. P. de-Matos, D. Nowell, M. J. Pavier, R. J. Paynter, D. J. Smith, S. Simandjuntak, International Journal of Fatigue, 29 (2007) 222.
[5] D. Damri, J. F. Knott, Fatigue and fracture of engineering materials and structures, 14(7) (1991) 709.
[6] G. Wheatley, X. Z. Hu, Fatigue and fracture of engineering materials and structures, 22(12) (1999) 1041.
[7] J. R. Rice, Fatigue Crack Propagation, ASTM STP. Philadelphia, (1967).

[8] S. Suresh, Engineering Fracture Mechanics, 18 (1983) 577.
[9] P. Lopez-Crespo, D. Camas-Peña, A. Gonzalez-Herrera, J. R. Yates, E. A. Patterson, J. Zapatero, Key Engineering Materials, 385-387 (2008) 369.
[10] R. Branco, D. M. Rodrigues, F. V. Antunes, Fatigue and fracture of engineering materials and structures, 31(2008) 209.
[11] A. Steuwer, J. Santisteban, M. Turski, P. J. Withers, T. Buslaps, Nucl Instr Meth Physics Research B, 238 (2005) 200.
[12] M. Croft, Z. Zhong, N. Jisrawi, I. Zakharchenko, R. L. Holtz, J. Skaritka, T. Fast, K. Sadananda, M. Lakshmipathy, T. Tsakalakos, International Journal of Fatigue, 27 (2005) 1408.
[13] A. Steuwer, M. Rahman, A. Shterenlikht, M. E. Fitzpatrick, L. Edwards, P. J. Withers, Acta Materialia, 58 (2010) 4039.
[14] ASTM E647 Standard Test Method for Measurement of Fatigue Crack Growth Rates. (2003).
[15] P. J. Withers, In: Analysis of Residual Stress by Diffraction using Neutron and Synchrotron Radiation, M E Fitzpatrick, A. Lodini editor, London: Taylor & Francis, (2003) 170.
[16] S. Suresh, Fatigue of Materials, Cambridge: Cambridge University Press, (2004).
[17] H. M. Westergaard, Journal of Applied Mechanics, 61 (1939) A49.
[18] F. Yusof, P. J. Withers, P. Lopez-Crespo Crack closure effect in near threshold fatigue crack growth perturbed by an overload cycle. Acta Materialia; To appear in 2011.